

**GEOLOGICAL MAP OF THE HUMBOLDTIANUM BASIN AND ITS DEPOSITS.** E. F. Schmidt<sup>1</sup> and P. D. Spudis<sup>2</sup>, <sup>1</sup>Department of Physics, Embry-Riddle Aeronautical University, 3700 Willow Creek Rd., Prescott, AZ 86301 (schmide2@my.erau.edu), <sup>2</sup>Lunar and Planetary Institute, 3600 Bay Area Blvd., Houston, TX 77058

**Introduction:** Humboldtianum is a Nectarian-age multi-ring basin centered at approximately 57° N, 82° E. The inner ring is roughly 275 km in diameter and the outer (main) ring is estimated at around 650 km in diameter [1]. Although the basin was previously studied and mapped [2], new image data from Lunar Reconnaissance Orbiter (LRO) and chemical and mineral concentration data from Clementine and Lunar Prospector provide improved image resolution and information on the composition of basin deposits, allowing updated geological maps to be compiled and new inferences made about the composition of basin ejecta and its crustal target.

The basin is asymmetric and morphologically complex; it is strongly polygonal in the south but irregular and chaotic in the north and east. Bel’kovich crater appears to overlie Humboldtianum’s inner ring in this area. The unusual shape of the basin may be indicative of its formation from an oblique impact, as has been proposed for some other basins [3].

The purpose of this project was to create a geological map centered on the Humboldtianum basin, allow-

ing a better understanding of the composition of its ejecta deposits and crustal target. In addition, compositional analysis was used to help determine the level of influence of the younger Imbrium and Crisium basins on Humboldtianum itself. This was done by mapping all the important units related to the basin, which included their relative ages, and looking for compositional clues as to their origin. The image data for this map comes from narrow-angle and wide-angle Lunar Reconnaissance Orbiter Cameras (LROC), the LRO GLD-100 topographic map [4], along with data on TiO<sub>2</sub> and FeO content from Clementine images [5] and thorium concentration data from Lunar Prospector [6]. This map can be used to help future lunar mission planning and in determining the basin target composition. In addition, the new mapping can help develop a better understanding of how Bel’kovich and Humboldtianum are related.

**Methods:** Basin-centered, orthographically projected LRO images and topographic maps were used in ArcGIS 10.1 to assist in the determination and mapping of the different stratigraphic units around the basin based on relative age, elevation changes, surface texture, albedo, FeO content (to help distinguish between plains and mare), and position. To improve comparisons and provide continuity with existing maps, mapping conventions were based on those of the 1978 USGS map of the lunar north side [2]. Only craters of greater than 20 km in diameter were mapped. After the new map was finished, compositional maps were overlaid onto it, allowing the concentrations of Fe, Ti, and Th to be determined for each geological unit and region of the basin and its surrounding area.

**Results:** A total of 23 geological units were mapped (Fig. 1), and divided into four categories: basin materials, other terra materials, mare and dark mantle materials, and crater deposits. Mapped units ranged from pre-Nectarian to Copernican. In addition, important non-stratigraphic geologic features were mapped, including large cracks in the Bel’kovich floor, the fault indicating the outer edge of the basin, the Compton-Bel’kovich thorium anomaly, and craters buried by basin and other crater ejecta. The results of the chemical composition data (Fe, Ti, and Th) are shown by region in Figure 2 below.

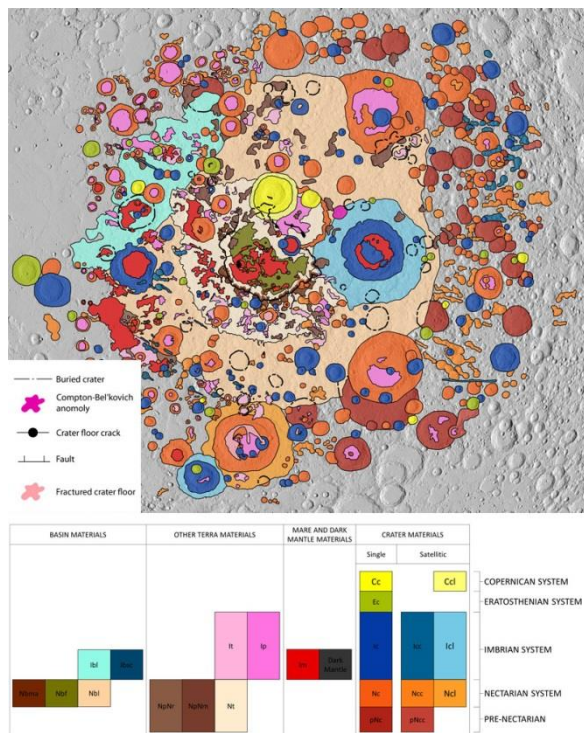


Figure 1 – New geological map of the Humboldtianum basin.

**Analysis:** On the basis of the data from Figure 2, although the uncertainties are large, a negative gradient in FeO content can be seen running from the north-west to the south-east, where the region mapped as Imbrium ejecta is the highest in Fe (most mafic). This suggests a slightly larger influence from Imbrium than is detectable from the mapping. However, due to the formation of subsequent large craters and mare flooding in the area, it is difficult to determine if this high FeO wt % is due solely to Imbrium ejecta or caused by inadvertent lumping of highland and mare units during analysis.

Although there is also a general negative trend in thorium concentrations heading east, a spike can be seen in the Compton ejecta and in the Bel'kovich region. This is caused by the Compton-Bel'kovich thorium anomaly, marked in bright pink Figure 1, which has a very high thorium content relative to the rest of the basin region ( $5.10 \pm 0.19$  ppm). This feature has been proposed as the site of the eruption of silicic volcanic rocks (i.e., rhyolite), a very rare phenomenon on the Moon [7].

Other than the high concentrations of FeO in the dark mantle and mare, the other units are all of feldspathic highlands composition, with little variation. Compared with the composition of the other basins previously studied [8-11], Humboldtium ejecta is relatively low in FeO, even lower than Orientale, which is very iron-poor [9]. This result suggests that the ejecta from Humboldtium is extremely feldspathic and the basin crustal target likely consisted of very ancient anorthositic rocks, which appear common in the northern central far side highlands [12].

The TiO<sub>2</sub> content of the ejecta is fairly uniform throughout the region with the notable exceptions of Compton-Bel'kovich and the terra material (Nt) inside Bel'kovich. The low concentration of TiO<sub>2</sub> inside Bel'kovich (~0.1 wt. %; Fig. 2) might reflect the presence locally of very feldspathic rocks.

The average elevation south of the basin is much higher than the average elevation north of it such that the peaks of the northern massifs are approximately equal in elevation as the southern highlands. Moreover, many massifs exist in the northern areas but not in the southern. One possible explanation for this relation is that the basin-forming impact hit in a northerly direction at a highly oblique angle. It should be noted that the highest elevation in the south is approximately the same as the peaks of the massifs in the north.

Compared with other recently mapped basins, Imbrium, Orientale, and Crisium [9-11], Humboldtium contains lower levels of Ti and, on average, lower levels of Fe. Notably, impact melt deposits were not found during the mapping. This is either because they

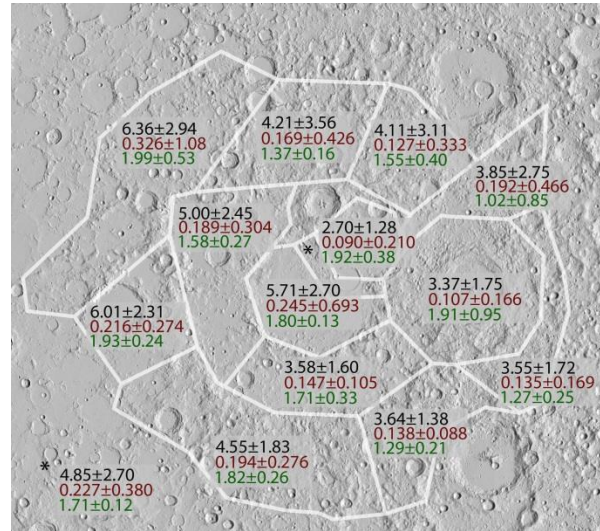


Figure 2 – Elemental composition of Humboldtium basin units. Black = FeO wt. %; Brown = TiO<sub>2</sub> wt. %; Green = Th ppm.

do not exist or are now covered by younger geological units (e.g., mare and crater deposits).

**Conclusions:** A new geological map of the Humboldtium basin was created using new data from the LRO, Clementine, and Lunar Prospector missions. The chemical data was related to mapped ejecta units around the basin, and stratigraphic units were recorded and analyzed. Analysis shows that the different basin units have similar compositions. However, there was a noticeable difference in FeO content in the different regions of the basin, a negative content gradient was found to exist from the north-west to the south-east. This suggests that there is a large Imbrium-basin influence on that side of Humboldtium but much less, if any, influence on the side away from the Imbrium basin. It was also found that large massifs are north of the basin while the region to the south is more uniform in elevation, with fewer massifs present.

**References:** [1] Wilhelms, D. E. (1987) *The Geologic History of the Moon*. USGS Prof. Paper 1348, 302 pp. [2] Lucchitta, B. K. USGS map I-1062. [3] Schultz, P. H., Crawford, D. A. (2016) doi:10.1038/nature18278 [4] Scholten, F. et al. (2012) doi:10.1029/2011je003926 [5] Lucey P.G. et al. (2000) JGR 105, 20297. [6] Lawrence D. et al. (2007) GRL 34, L03201, doi:10.1029/2006GL028530. [7] Jolliff, B. L. et al. (2011) LPSC. [8] Smith, M. C., Spudis, P. D. (2013) LPSC. [9] Martin, D. J. P., Spudis, P. D. (2014) LPSC [10] Murl, J. N., Spudis, P. D. (2015) LPSC [11] Sliz, M. U., Spudis, P. D. (2016) LPSC. [12] Jolliff, B. L. et al. (2000) JGR 105, 4197.